

Magneto-Absorption Spectra of One-Dimensional Ising Antiferromagnets in High Magnetic Fields(Magneto-optics)

著者	Takeda Masayasu, Mogi Iwao, Kido Giyuu, Nakagawa Yasuaki
journal or publication title	Science reports of the Research Institutes, Tohoku University. Ser. A, Physics, chemistry and metallurgy
volume	38
number	2
page range	269-278
year	1993-06-30
URL	http://hdl.handle.net/10097/28444

Magneto-Absorption Spectra of One-Dimensional Ising Antiferromagnets in High Magnetic Fields*

Masayasu Takeda **, Iwao Mogi , Giyuu Kido and Yasuaki Nakagawa

Institute for Materials Research, Tohoku University, Sendai

(Received January 19, 1993)

Synopsis

We have performed magneto-absorption spectra measurements of the quasi-one-dimensional antiferromagnet $\text{RbFeCl}_3 \cdot 2\text{H}_2\text{O}$ with a hybrid magnet installed at High Field Laboratory for Superconducting Materials in Tohoku University.

I. Introduction

Magneto-absorption measurement is one of useful technics to investigate the 3d transition metal insulators because the absorption spectra contain information on not only electronic excitations but also magnetic excitations [1]. Magneto-absorption spectra have been intensively investigated in Heisenberg or XY magnets up to now. However there are few works on Ising antiferromagnets. Among them a one-dimensional (1D) Ising antiferromagnet shows unique physical properties due to the 1D character and the strong anisotropy. For example antiphase boundaries are excited by thermal energy and freely propagate in the linear chain. This antiphase boundary is known to be a domain wall soliton. In this paper we report the study of exciton of a 1D Ising antiferromagnet $\text{RbFeCl}_3 \cdot 2\text{H}_2\text{O}$ and how the character of 1D Ising antiferromagnet reflects on the absorption spectra.

II. Magnetic Structures and Magnetic Properties of $\text{RbFeCl}_3 \cdot 2\text{H}_2\text{O}$

$\text{RbFeCl}_3 \cdot 2\text{H}_2\text{O}$ (RFC) is regarded as a quasi-one-dimensional canted Ising antiferromagnet [2]. The magnetic chains consist of antiferromagnetic spins lining along the orthorhombic a -axis. The intrachain interactions ($J_a = -39$ K in the $S=1/2$ formalism) are two orders of magnitude larger than the interchain ones ($J_b =$

* The 1929th report of Institute for Materials Research

**Present address : Department of Physics, Faculty of Science, Tohoku University, Sendai

-0.76 K, $J_c = -0.21$ K) [3]. Below the Néel temperature ($T_N=12.6$ K) the small interchain interactions lead to three dimensional magnetic order as shown in Fig 1 (a). In this state all spins are within the ac - plane and make an angle of 19° from the a -axis, so that each chain has weak ferromagnetic moments in the direction of the c -axis. These moments couple with the nearest neighbor chains ferromagnetically in the direction of the c -axis, but antiferromagnetically in the b direction. In this magnetic structure external magnetic fields along the a -axis and the c -axis are expected to induce the magnetic phase transition from antiferromagnetic state to the forced ferromagnetic one. Spin structures in the forced ferromagnetic phases of the two cases are illustrated in Fig. 1 (b) and (c), respectively.

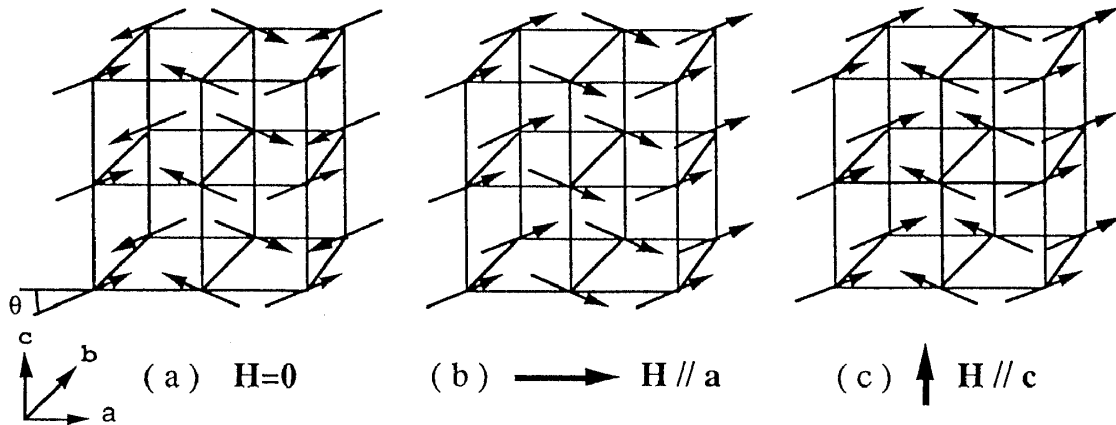


Fig. 1 Spin structures of $\text{RbFeCl}_3 \cdot 2\text{H}_2\text{O}$ below T_N , (a) in the absence of a magnetic field, (b) after the phase transition under the fields along the a -axis and (c) after the transition in the fields along the c -axis.

III. Experimental

Single crystals of $\text{RbFeCl}_3 \cdot 2\text{H}_2\text{O}$ were grown by slow evaporation of an aqueous solution of RbCl and $\text{FeCl}_2 \cdot 4\text{H}_2\text{O}$ in the molar ratio 1:3.2. The plates with the crystal face of the ab -plane were obtained, and the samples used in the experiments were typically $3 \times 3 \times 0.5$ mm³.

Magneto-absorption spectra measurements in high magnetic fields were performed by using a hybrid magnet HM-2. A Xenon short-arc lamp and an interference filter (Melles Griot, 03FIB002) were used as the light source with a band width of 80 nm. The incident light was polarized linearly by a Polaroid sheet (HNP'B) before a sample. The transmitted light through the sample was introduced into a polychromator (JOBIN YVON, THR 1000S, $f=8.4$, 1200 grooves/mm) by an optical fiber and detected in the second order harmonics by a photodiode linear

sensor (Hamamatsu Photonics K. K., S2304-1024Q). A Ne lamp (Toshiba, HSL-Ne-1) was used for calibration. The resolution was approximately 2 cm^{-1} when the entrance slit was open in $100 \mu\text{m}$ width. Temperature was stabilized by a capacitance controller (Lakeshore, CSC400) within $\pm 0.1 \text{ K}$. Details of this apparatus and the performance were reported in the other paper [4].

Magnetization curves at 4.2 K up to 23 T were measured by a sample extraction magnetometer attached to the HM-2. Magnetization measurements at various temperatures up to 14 T were done with a vibrating sample magnetometer by using WM-5.

IV. Results

Magnetization processes of RFC at 4.2 K are plotted in Fig. 2 (a) when magnetic fields are applied parallel to the three principal axes. When magnetic fields are applied parallel to the a -axis, the magnetization effectively increases in the field region between 10 T and 15 T . The value of the magnetic moments reaches $4.2 \mu_{\text{B}}/\text{Fe}^{2+}$ at 23 T , which is a little larger than the expected magnetic moments of Fe^{2+} if orbital magnetic moments were completely quenched. This indicates that the spin configuration illustrated in Fig. 1 (b) are realized in the fields higher than 15 T . The metamagnetic transition (Fig. 1 (a) \rightarrow (c)) was observed at around 1 T in the field parallel to the c -axis. In the direction of the b -axis the magnetization monotonically increases with increasing fields as expected from the magnetic structure. The phase transitions proceed more slowly above the Néel temperature at 14 K as shown in Fig. 2 (b).

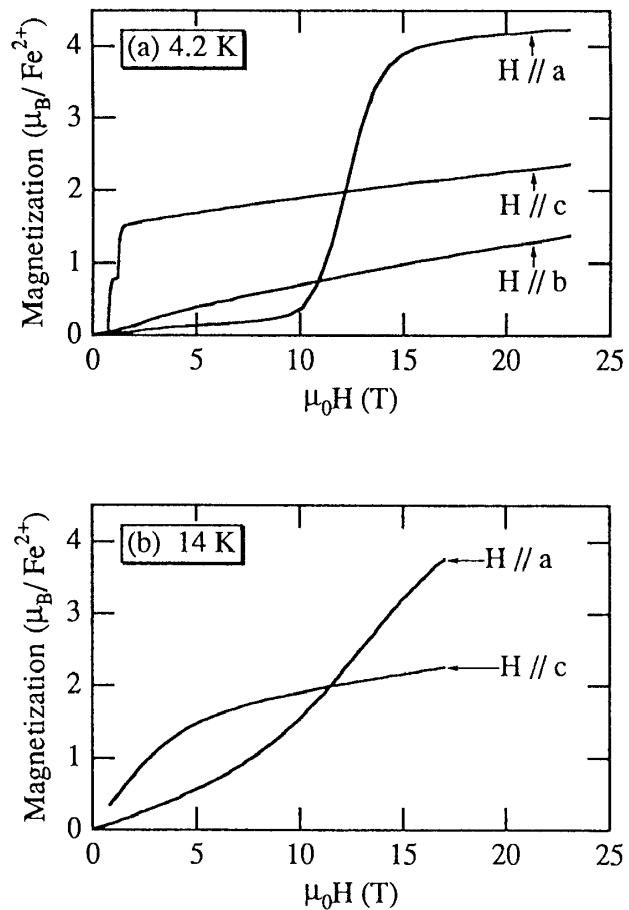


Fig. 2 Magnetization processes at 4.2 K along the three principle orthorhombic axes (a) and at 14 K along the a - and the c -axis (b), respectively.

Figure 3 shows the magnetic field dependence of the absorption spectra of RFC in the magnetic fields along the a -axis with the electric field vector of the incident light \vec{E} parallel to three principal axes, respectively. The spectra in three different magnetic states are displayed in these figures, i.e. in the antiferromagnetic state at 0 T, the state at the midpoint of the transition and the forced ferromagnetic state at 23 T. The intensity of each absorption line can be compared with each other under the same polarization condition. The spectra under the different polarization conditions, however, have not been normalized. The spectra are remarkably changed by the magnetic phase transition, which indicates that the absorption lines are very sensitive to the spin configuration.

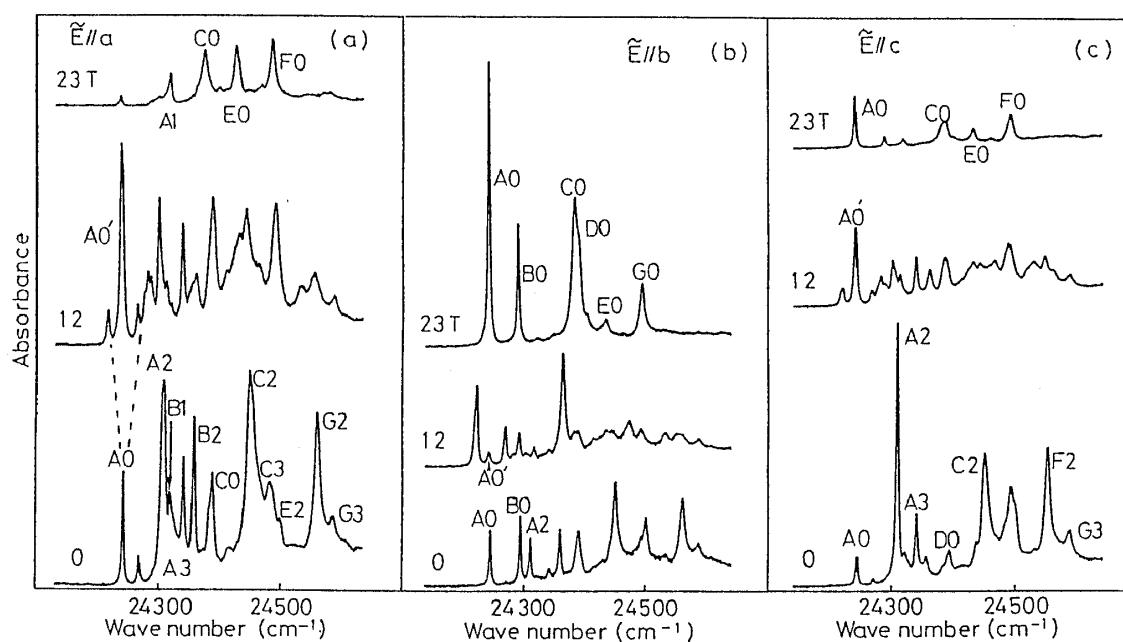


Fig. 3 Magneto-absorption spectra of $\text{RbFeCl}_3 \cdot 2\text{H}_2\text{O}$ at 4.2 K with polarizations (a) $\vec{E} // a$, (b) $\vec{E} // b$ and (c) $\vec{E} // c$.

The absorption lines in this energy region are due to the d-d transition of Fe^{2+} from ${}^5\text{T}_2(\text{D})$ to the overlapped region of ${}^3\text{T}_2(\text{G})$, ${}^3\text{A}_2(\text{F})$ and ${}^3\text{T}_1(\text{F})$ in the cubic approximation, and all of the transitions are spin forbidden [5]. The absorption lines appearing in this energy region are classified into several groups [6]. Each group has an exciton line and its sidebands. These groups are overlapped in the higher energy region of Fig. 3. The fine structures of the spectra are very similar to that of isomorphous compounds $\text{CsFeCl}_3 \cdot 2\text{H}_2\text{O}$ (CFC) because the octahedron around Fe^{2+} , $\text{cis-}[\text{Fe}(\text{H}_2\text{O})_2\text{Cl}_4]$, is common in these two compounds. The groups with the lowest excitation energy in the fine structures of CFC have been assigned in ref 7, and the same assignment can be valid for RFC.

An absorption line labeled A0 is an exciton line in the antiferromagnetic state.

The A1, A2 and A3 lines are the magnon sidebands of the A0 line. These sidebands show anomalous behavior in the magnetic fields. For instance, the lower branch of the A1 line crosses over the higher energy branch of the A0 line at 8 T due to the magnetic Franck-Condon effect [6, 8]. The other properties of these sidebands are reported in ref 6. The same relation of the notation holds on the other groups (B0, B1, B2 etc.) in which the notation is based on the energy separation between the absorption line labeled 0 and its sidebands. In the following section, we concentrate on the A0 exciton line.

The A0 line is observed in the antiferromagnetic phase with all three polarizations. It shows sublattice splitting in the magnetic fields up to 15 T. The magnitude of the splitting linearly increases with increasing magnetic fields. The splittings are no longer detected in the field higher than 15 T. Instead of the splitting of the A0 line, an absorption line which shifts to the higher energy side is weakly observed with $\tilde{E} // a$, and the intensity of the line is enhanced with $\tilde{E} // b$ in the forced ferromagnetic phase.

In the vicinity of 12 T, an extra line denoted as A0' is clearly observed between two A0 branches with $\tilde{E} // a$ and $\tilde{E} // c$. The line shifts to the higher energy side with increasing magnetic fields. The intensities of the A0' line observed in $\tilde{E} // a$ are plotted as a function of the magnetic fields in Fig. 4. The intensity of the extra line has the maximum value at 12 T and can be detected neither in the antiferromagnetic phase nor in the forced ferromagnetic one. The solid line in Fig. 4 is the calculation within the framework of the one-dimensional Ising model which is described in the next section.

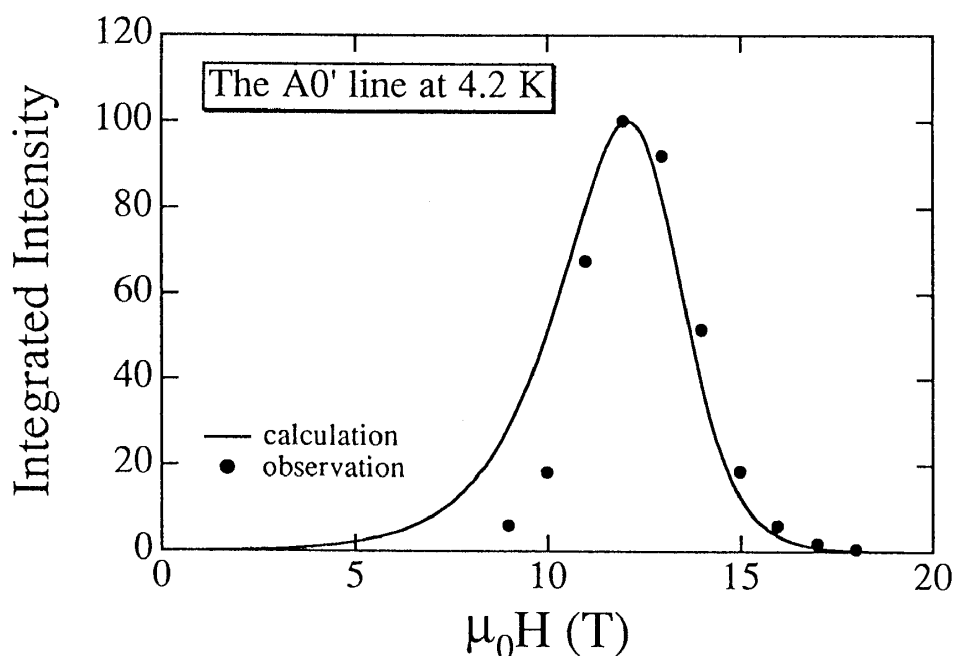


Fig. 4 Integrated intensity of the A0' line as a function of applied field. The solid line is the calculation within the framework of the one-dimensional Ising model.

Magneto-absorption spectra of RFC at 14 K in various magnetic fields parallel to the a -axis are shown in Fig. 5 (a). In this figure the spectra in $\vec{E} // a$ polarization are only shown. Several new lines appear as hotbands in this figure. Here we pay attention to the HA0 line which has the lowest excitation energy in these fine structures. The HA0 line can be detected above 10 K in the lower energy side of the A0 line with energy separation of $|J_a|$ at 0 T.

In magnetic fields the HA0 line shows the sublattice splitting. While the intensity of the higher branch takes a maximum value at 12 T, that of the lower branch monotonically decreases with increasing fields. In the forced ferromagnetic state the HA0 line is not detected. The intensities of the HA0 line are plotted as a function of temperature and of a magnetic field in Fig. 6 (a) and (b), respectively. In these figures the solid lines by the same calculation as used in the analyses of the A0' line are also drawn. It is clearly seen that the HA0 line significantly loses its intensity below the Néel temperature.

Figure 5 (b) shows the magnetic field dependence of the HA0 line with $\vec{E} // a$ polarization in the fields parallel to the c -axis at 14 K. Magnetic fields in this direction causes sublattice splitting of the HA0 line due to the weak ferromagnetic moments. The intensity of the higher branch is stronger than that of the lower one. The intensities of both branches decrease with increasing fields and are drastically suppressed in the fields between 2 T and 4 T. When the external magnetic fields are applied parallel to the c -axis, the metamagnetic transition of the weak ferromagnetic moment takes place in the field region between 2 T and 4 T at 14 K as shown in Fig. 3 (b). It is clear that the suppression of the HA0 line has a close relation with the phase transition.

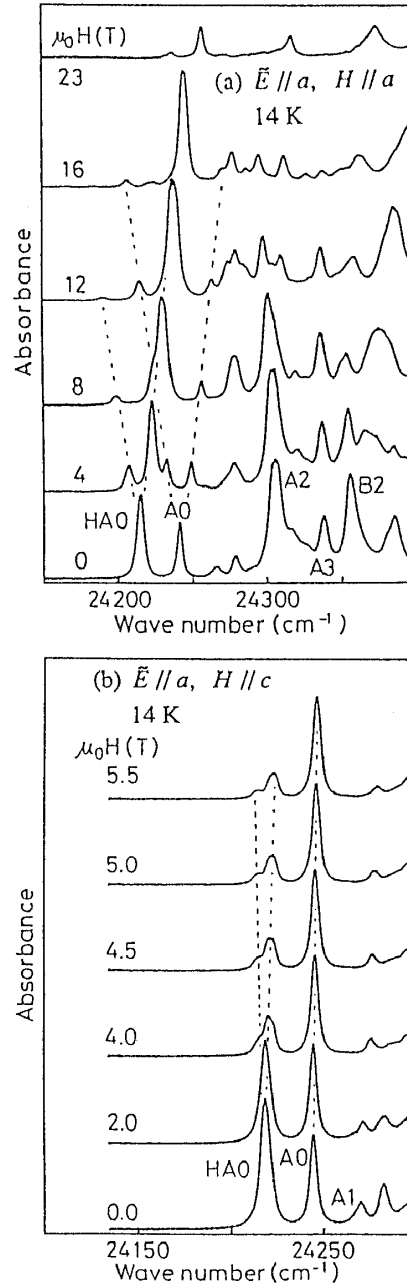


Fig. 5 Absorption spectra with a polarization $\vec{E} // a$ at various magnetic fields along (a) the a -axis and (b) the c -axis at 14 K.

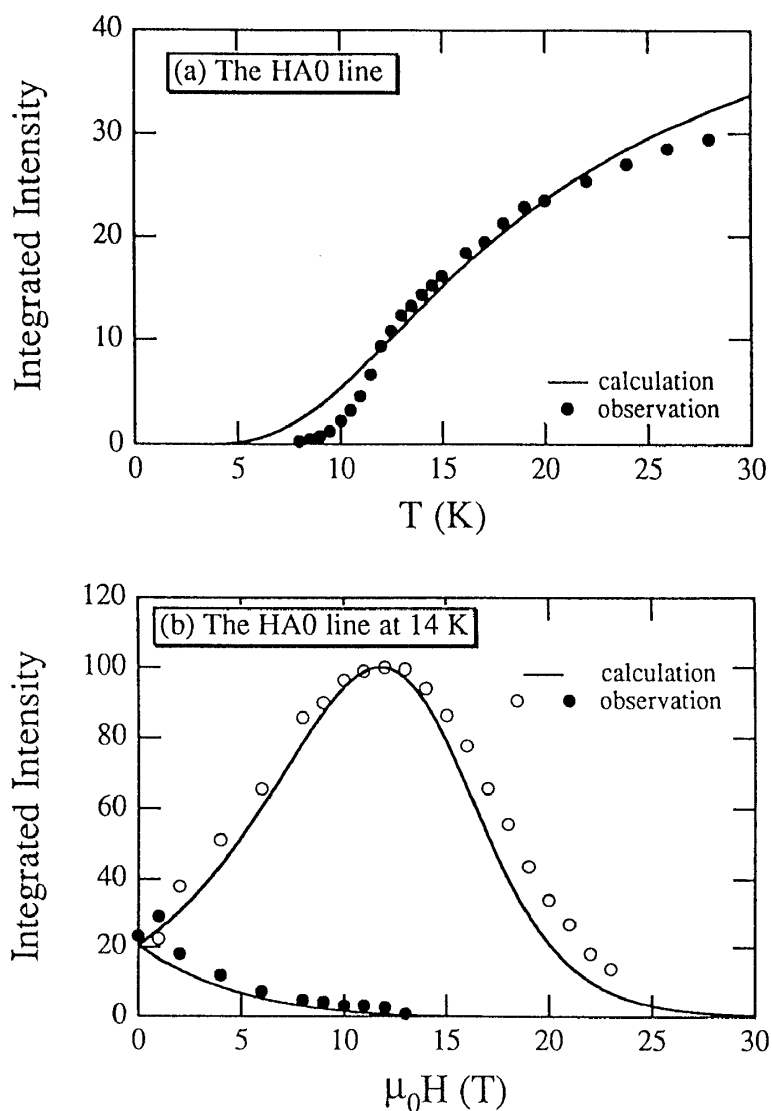


Fig. 6 The temperature dependence of the intensity of the HAO line (a) and the magnetic field dependence of two branches of the HAO line (b). The solid lines are the calculation with the same parameters used in Fig. 4

V. Discussion

The electronic excitation of d-d transition in 3d magnetic insulators are usually described as Frenkel exciton. The exciton often couples magnons and phonons, and magnon sidebands or phonon sidebands appear in the fine structure of light absorption spectra. However, there are several cases that the electronic excitation has a local excitation character. In RFC the A0 line is described as the local excitation rather than the exciton because Davydov splitting is unobserved.

The ground state of the A0 line is the lowest doublet which originates from the splitting of $^5D(3d^6)$ state by the crystal field and the spin-orbit interaction. The degeneracy is removed by the antiferromagnetic exchange interaction even in the absence of the magnetic fields. The ground state of the A0 line is one of this doublet which has up or down spin according to the sublattice in the linear chain. The magnetic fields make the energy difference of sublattice by amount of the Zeeman energy. On the other hand, the excited state of the A0 line is a singlet state, so that the energy level of the excited state is insensitive to the magnetic fields. Linearity of the sublattice splitting of the A0 line can be understood by these explanation. In the forced ferromagnetic phase the antiferromagnetic sublattice no longer exists, and the lowest energy level of each site is the same. The absorption line whose ground state is this level is clearly observed with $\vec{E} // b$ in the forced ferromagnetic phase and shifts to the higher energy side with increasing magnetic fields as shown in Fig. 3.

The energy levels of Ising spins in the antiferromagnetic chain and the corresponding spin configurations are schematically illustrated in Fig. 7. In this figure the chain is running horizontally, and the easy axis of the Ising spins is perpendicular to the chain. When the only exchange interaction between the nearest neighbor spins is considered, the energy state of each spin splits into six energy levels [(a) ~ (f) in Fig. 7] in an external magnetic field parallel to the easy axis. The A0 line is represented by the arrow which starts at the degenerated levels [(a) and (b)] in the figure. The absorption line in the forced ferromagnetic state should be described by the arrow which starts at (f) level and ends at the same excited state as the A0 line.

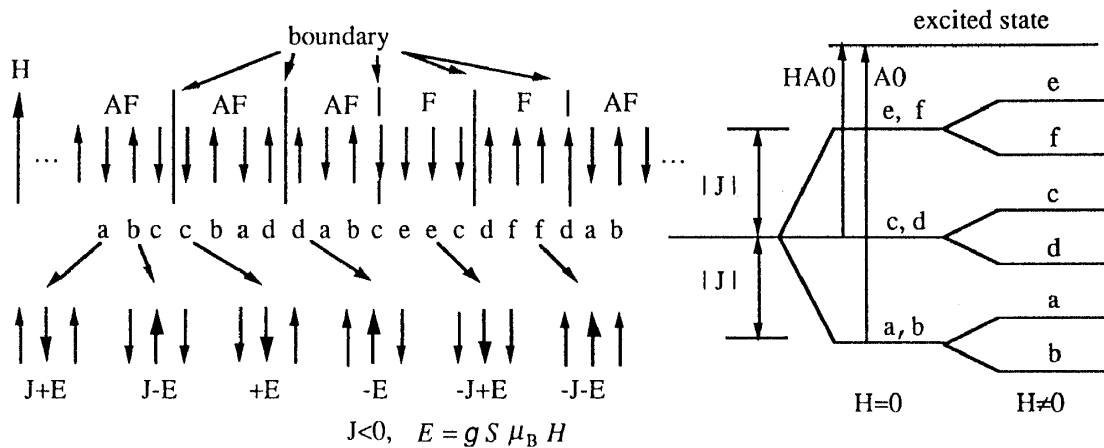


Fig. 7 Schematic representation of the arrangement of the Ising spins in the antiferromagnetic chain and the energy levels of six different spins in different local configurations. Each spin is named (a) ~ (f), respectively. Energy scheme of the A0 and the HA0 lines (see text) is also drawn in this figure.

The phase transition from the antiferromagnetic to the forced ferromagnetic phase in the a - axis is caused by the flipping of the Ising spins parallel to the external magnetic fields. There are two kinds of process of the flipping. One is the

flipping of the whole spins which belong to the same chain at one time, and the other is the gradual flipping of local spins in the chain. When the transition process is dominated by the flipping of local spins, the site at which exchange interactions are canceled out [(d) site in Fig. 7] should exist in one chain during the transition process. The absorption line whose ground state is the (d) level and excited state is the same as the A0 line appears during the phase transition process and has to disappear in both the antiferromagnetic phase and the forced ferromagnetic one.

The A0' line in Fig. 3 can quantitatively be regarded as an absorption line at the (d) site. If this assignment is valid, the intensity of the A0' line should be proportional to the number of the (d) site in Fig. 7. The solid line in Fig. 4 is the calculation of the magnetic field dependence of the number of (d) site within the framework of the one-dimensional Ising model. The calculation and the observation are normalized by each maximum values. The parameters used in the calculation, exchange interaction and saturation magnetization, are determined by the energy shift of the A0 and the A1 line and the magnetization measurement, respectively. The calculation well reproduces the observation. In addition to this, the magnitude of the energy shift can be also reproduced by another calculation which was described in detail in ref. 6. It can be concluded that the A0' line is the electronic excitation at the site on the boundary between antiferromagnetic and the ferromagnetic regions in the linear chain created during the phase transition process. The small difference between the calculation and the observation in Fig. 4 is due to the small interchain interactions.

RFC can be regarded as a 1D Ising antiferromagnet above the Néel temperature. In the temperature region antiphase boundaries, soliton, are created in the linear chain. It should be noted that the exchange interaction is canceled out at the (c) and (d) sites which are next to the soliton as shown in Fig. 7. The HA0 line can be assigned to the electronic excitation at the (c) or (d) site with the same excited state as the A0 line. This assignment is supported by the calculation of the magnitude of the sublattice splitting and the number of the (c) and (d) site as a function of temperature and the magnetic fields as shown in Fig. 6. The calculation has been done by the same values of parameters as used in Fig. 4. It is clearly seen that the antiferromagnetic spin configuration is stabilized and the creation of the soliton is suppressed by the interchain interactions.

The weak ferromagnetic moment (WFM) of the Ising chains is ignored in the above discussions. It is important that the (c) and (d) sites are created whenever the WFM is flipped because the component of Ising spins parallel to the a -axis flips at the sites where the WFM flips. When the external magnetic fields are applied parallel to the c -axis, the metamagnetic transition of the WFM takes place, and the spin configuration illustrated in Fig. 1 (c) is realized in the fields higher than 2T at 4.2 K as shown in Fig. 2 (a). The HA0 line shows the sublattice splitting in this field direction (Fig. 5 (b)). It arises from the fact that the WFM of two sites next to the soliton is opposite to each other. As shown in Fig. 2 (b) almost all of the WFM is parallel to the field direction in fields higher than 4 T. In this state some WFM must be flipped to the opposite direction to the field when the solitons are created in the

chain. Hence the intensities of the two branches in the HA0 line significantly decrease between 2 T and 4 T [9]. In chains whose WFM is parallel to the magnetic field, flipping of only one spin is dominant because the larger antiferromagnetic region flip in the chain, the more Zeeman energy is required. While the excitation of soliton creates one pair of the exchange-cancelled-sites whose WFM is parallel and antiparallel to the magnetic fields, the one-spin-flip creates two exchange-cancelled-sites whose WFM is parallel to the fields. This causes the unbalance of the intensities of two branches.

In conclusion we have studied the phase transition process and the antiphase boundary in the 1D Ising antiferromagnet $\text{RbFeCl}_3 \cdot 2\text{H}_2\text{O}$ through the investigation of exciton lines using the fact that the ground states of the excitons depend on the local configuration of spins in the linear chain.

The authors are much indebted to all staff members in High Field Laboratory for Superconducting Materials for the operation of the hybrid magnet. Thanks are also due to the members in Cryogenic Center of Tohoku University for assistances in cryogenic aspects. This work was partly supported by Grant-in-Aid for Scientific Research of Ministry of Education, Science and Culture, Japan.

References

- [1] V.V. Eremenko, Yu. G. Litiviinenko and E. V. Matyushkin, *Phys. Rep.* **2** (1986) 55.
- [2] J. A. Basten, Q. A. G. Vlimmeren and W. J. M. de Jonge, *Phys. Rev.* **B18** (1978) 2179.
- [3] J. P. M. Smeets, E. Frikkee, W. J. M. de Jonge and K. Kopinga, *Phys. Rev.* **B31** (1985) 7323.
- [4] G. Kido, I. Mogi, M. Takeda and Y. Nakagawa, *Physica* **B164** (1990) 76.
- [5] M. Takeda, I. Mogi, G. Kido and Y. Nakagawa, *Physica* **B177** (1992) 368.
- [6] M. Takeda. Dr. Thesis, Tohoku University (1991) .
- [7] H. Okada, N. Kojima, T. Ban and I. Tsujikawa, *Phys Rev.* **B18** (1990) 11610, *ibid.***B18** (1990) 11619.
- [8] I. Mogi, M. Takeda, G. Kido, Y. Nakagawa, H. Okada and N. Kojima, *J. Magn. Magn. Mater.* **104-107** (1992) 1061.
- [9] M. Takeda, I. Mogi, G. Kido, Y. Nakagawa, H. Okada and N. Kojima, *J. Magn. Magn. Mater.* **90&91** (1990) 244.